Methodological Approach for Understanding Particle Transport. Case Study: Analyzing Influential Factors and Comparing Simulation Software

Cornelia Müssig[1], Alexander Kabat vel Job[2], Dr.- Ing. Stephan Knorr[2], Prof. Dr.- Ing. Henning Meyer[1], Prof. Dr.- Ing. Daniel Wiest[1]

[1] Chair of Machinery System Design, Technical University of Berlin (TU Berlin), Berlin, Germany
[2] Volkswagen AG, Wolfsburg, Germany
Correspondence: cornelia.muessig@tu-berlin.de

Abstract

Recent research shows that the investigation of particle flow of small particles with diameters smaller than 10 micrometers has emerged as an important field of interest, especially for purposes in the industrial sector. Investigating the behavior, deposition and acting forces of individual particles have become particularly relevant. Understanding theses dynamics is crucial for setting up practical simulations in terms of particle transport drawn from industrial problems. Previous research has identified numerous forces involved in particle transport e.g. Sommerfeld, 2000, Crown, 2005, Löffler & Raasch, 1992 or Crown, et al., 2011. However, not all of the various forces have yet been implemented in practice for different reasons.

In this case study, acting forces are examined theoretically using a component coming directly from the automotive industry. The examined component is a venting tube used in headlights of vehicles. Due to its simple geometry the component is suitable for investigating particle-laden flow using different simulation software. The simulation setup for this component is less complex, which saves time and reduces computational costs. The implementation of the examination processes within different types of simulation software has been analyzed too.

Simulating a particle-laden flow results in significant computational costs. It is therefore necessary to identify and implement boundary conditions. All results serve as the basis for developing an appropriate simulation model and to create a methodological approach representing particle transport. The simulation results have been validated using suitable experiments. Furthermore, a transfer function is derived to determine the filtering effect of the mentioned automotive component. This study combines theoretical background with a practical approach.

Keywords

methodological approach, particle transport, particle-laden flow, industrial example, transfer function, filtering effect

Introduction

Modern automotive headlights need to be ventilated to remove humidity from the housing and to prevent condensation on optical surfaces. The ventilation in headlights also enables dust to enter the system. To reduce the inflow of dust, venting tubes are assembled at the headlights. They allow a controlled air inflow to transport the moisture out of the housing, while at the same time filtering dust particles. The following sections will give details of the airflow through venting tubes and their particle transport.

Particle-laden flows represent a complex multiphase problem that remains difficult to predict in technical systems. Their behavior is mainly influenced by the inertia, drag, as well as wall and particle interactions, which also strongly depends on the particle size. As headlights are sealed systems, direct experimental measurement of particle penetration is not possible without damaging the components. Thus, numerical simulations and simplified physical models are used as tools to investigate the behavior.

While previous research developed a range of theoretical models and numerical methods for describing particle transport, two key challenges remain. First, fully resolved simulations are computationally demanding and solver-depending. Second, finding accurate boundary conditions, because they are essential to ensure a simulation setup. Experimental studies on real headlights are difficult due to inaccessibility. These limitations highlight the need for a controlled experimental setup combined with numerical approaches, which is also part of this study.

The objective of this study is to investigate the dust filtration behavior of venting tubes. Two numerical tools, Meshfree and STAR-CCM+, were used to simulate airflow and particle transport based on distinct numerical formulations (Eulerian vs. Lagrangian). Their results are compared with experimental data.

The experiment allows systematic variation of boundary conditions. After each test run the dust was collected and analyzed in terms of their particle size distribution to quantify potential changes in the distribution and to detect the filtering effect of the venting tubes.

The structure of this paper is as follows: first the theoretical background of particle-laden flows and the relevant acting forces are presented. Followed by describing the applied methods and boundary conditions, including solver configurations and particle injection strategies. Later the implementation of the simulation tools is introduced, and details of the experimental setup and measurement procedure are given. The results from both simulations and experiments are discussed. Main findings are being summarizes and an outlook on future work is provided.

Theoretical background

The reliable prediction of particle-laden flows requires a solid understanding of the fundamental physical mechanisms. In technical systems, such as automotive venting tubes, these interactions determine whether particles can follow the main airflow, adhere to surfaces, or are filtered. Since particle behavior is strongly influenced by size, density, and flow conditions, a theoretical framework is necessary to establish appropriate simulation models and to interpret the results of experiments.

Stieß (2009) provided a systematic classification of the relevant mechanism. He describes the particle motion as a result of a superposition of distinct external forces. According to this framework, the following forces are typically considered as (Stieß, 2009, p. 213 ff.):

$$m_\mathrm{p} \cdot \frac{\mathrm{d}u_\mathrm{p}}{\mathrm{d}t} = \sum F_\mathrm{ext} \qquad (1)$$

The particle mass is represented with m_p and the particle velocity with u_p. The external forces (F_ext) are acting on the particle. The dominant external forces for particles in airflows are:

- **Drag force $\boldsymbol{F_\mathrm{D}}$**: resistance acting opposite to the relative velocity between particle and fluid.
- **Gravity force $\boldsymbol{F_\mathrm{G}}$:** Acting downward due to particle mass.
- **Buoyancy force $\boldsymbol{F_\mathrm{B}}$:** Resulting from pressure gradients in the flow field.
- **Added mass force $\boldsymbol{F_\mathrm{A}}$:** used for the acceleration of the surrounding fluid displaced by the particle.
- **Basset force $\boldsymbol{F_\mathrm{H}}$:** acting for unsteady viscous effects based on the particle's acceleration.
- **Inertial force $\boldsymbol{F_\mathrm{Tr}}$:** expressing the unsteady effects of the particle's own acceleration relative to the surrounding flow field.

These forces together describe the Basset–Boussinesq–Oseen (BBO) equation, which provides a general formulation for describing the unsteady motion of small spherical particles in a viscous fluid (Maxey & Riley, 1983; Michaelides, 1997).

$$m_\mathrm{p} \cdot \frac{\mathrm{d}u_\mathrm{p}}{\mathrm{d}t} = F_\mathrm{D} + F_\mathrm{A} + F_\mathrm{B} + F_\mathrm{G} + F_\mathrm{H} + F_\mathrm{Tr} + F_\mathrm{add} \qquad (2)$$

This expression represents the dynamic equilibrium between the particle's acceleration and the total sum of all external forces acting on it. Depending on the flow conditions and particle size, certain forces, such as the Basset term, may be neglected, while drag and gravity often dominate the particle motion under steady conditions (Stieß, 2009). Although a wide range of additional forces may influence the particle transport, such as electrostatics, thermophoretic effects or inter-particle collisions, they are, due to their complexity and minor relevance, not part of the present study.

The BBO formulation provides the theoretical basis for analyzing the Eulerian and Lagrangian approaches, which represent two principal methods in computational fluid dynamics (CFD) for modeling dispersed multiphase and particle-laden flows. Both differ fundamentally in how they represent the dispersed phase and its interaction with the carrier fluid. Further information about the Eulerian and Lagrangian formulation are explained in the section *Methods and boundary conditions* (p. 3).

Another important aspect of this study is the determination of the filtering effect of venting tubes through a transfer function. In classic transport theory it is defined as the normalized ratio between output and input quantities. It describes the relative transmissivity or efficiency of a system. Such formulations are widely applied in mass and momentum transport analysis to express how an initial distribution changes as it passes through a medium (Cussler, 2009).

Since the absolute particle concentrations before and after the venting tube are not known, only relative values based on the cumulative volume distribution $Q_3(x)$ are used. A transfer function $T(x)$ is in this case defined as the ratio of the input to the output cumulative volume distribution:

$$T(x) = \frac{Q_{3,\mathrm{out}}(x)}{Q_{3,\mathrm{in}}(x)} \tag{3}$$

$Q_{3,\mathrm{in}}(x)$ represents the input distribution (dust from the dust chamber) and $Q_{3,\mathrm{out}}(x)$ the output distribution (dust from the acrylic box with the applied venting tube). This ratio provides a dimensionless measure of particle transmission probability as a function of particle diameter.

A value of $T(x) = 1$ indicates complete particle passage through the venting tube, whereas $T(x) < 1$ reflects a filtering effect, meaning that parts of a specific particle size is filtered within the venting tube.

Although the function is based on relative values, it serves as a method to compare experimental and numerical results. As noted by Crowe et al. (2012), normalized or dimensionless parameters are particularly useful for comparing experimental and numerical results when absolute concentrations or mass fluxes cannot be measured directly.

Methods and boundary conditions

The following section describes the used methods and boundary conditions for the implementation of the simulation programs. Both simulation programs, Meshfree (Fraunhofer Institute) and STAR-CCM+ (Siemens), were configurated under the same physical assumptions to ensure a direct comparability of their results and to evaluate their predictive capability regarding particle transport and filtration behavior.

Both models use a one-way coupling approach, meaning that the airflow field affects the particle motion, while the particles do not influence the fluid phase. This assumption is valid for the present case since the particle volume fraction and particle size (< 10 µm) are small enough, making the momentum exchange between the dispersed and continuous phases considered as insignificant.

The motion of the particles in both solvers is based on a simplified form of the BBO equation (mentioned in the previous section, page 2). In this reduced form, only the dominant forces, drag, gravity, and buoyancy, are considered. The other terms such as added mass or the Basset force are not implemented. This simplification is justified by the quasi-steady flow conditions and the low particle–fluid density ratio. The resulting equation of motion is expressed as

$$m_\mathrm{p} \cdot \frac{\mathrm{d}u_\mathrm{p}}{\mathrm{d}t} = F_\mathrm{D} + F_\mathrm{G} + F_\mathrm{B} \tag{4}$$

The external forces acting on the particle are defined as:

$$F_\mathrm{D} = \frac{1}{2} \cdot C_\mathrm{D} \cdot \rho_\mathrm{f} \cdot A_\mathrm{p} \cdot \left|u_\mathrm{f} - u_\mathrm{p}\right| \cdot (u_\mathrm{f} - u_\mathrm{p}) \tag{5}$$

$$F_\mathrm{G} = m_\mathrm{p} \cdot g \tag{6}$$

$$F_\mathrm{B} = -V_\mathrm{p} \cdot \rho_\mathrm{f} \cdot g \tag{7}$$

with C_D as the drag coefficient, ρ_f as the fluid density, A_p as the particle cross-sectional area, V_p as the particle volume, and g as the gravitational acceleration vector (Stieß, 2009).

In the Eulerian framework used by Meshfree, the airflow field is discretized as a continuum, and particles are represented as concentrations. This approach allows efficient computation of flows with large particle populations and provides accurate predictions of mean concentration and transport fields. In contrast, the Lagrangian framework used in STAR-CCM+ explicitly tracks the path lines of individual particles within the airflow field. It allows a more detailed description of particle motion, wall collisions, and residence times. This method requires higher computational effort, particularly when simulating large particle numbers (Balachandar & Eaton, 2010).

The airflow was treated as laminar, incompressible, and steady, with an inlet velocity derived from the experimental volumetric flow rate ($\geq 1 \frac{\mathrm{l}}{\mathrm{min}}$ per venting tube). The outlet was defined as a constant static pressure boundary ($p = 0$ Pa), to ensure the mass conservation. All solid surfaces, including the inner walls of the venting tube, were modeled with no-slip conditions for the fluid and impermeable walls for the particle phase.

For both programs, the particle injection was determined in the same way - via a defined plan with a fixed grid at the inlet. This setup ensures that all particles have the identical position in each simulation to improve reproducibility and comparability between Meshfree and STAR-CCM+.

The particle injection time was selected so that the airflow field was already in a steady-state condition. In Meshfree, this was achieved immediately due to the use of a frozen steady-state field, whereas in STAR-CCM+ the

particles were injected only after the internally computed flow reached a steady state.

To ensure a consistent basis for comparison, identical particle material properties, size distributions, and wall boundary definitions were applied in both programs. Meshfree used an externally generated steady-state airflow field generated by OpenFOAM as a frozen background, while STAR-CCM+ computed the same airflow field internally under equivalent physical conditions. Any observed deviations between the simulation results can be attributed to the distinct numerical formulations rather than to variations in the physical setup.

Implementation of the software

The implementation of the simulation setup was realized using two computational tools, Meshfree (Fraunhofer Institute) and STAR-CCM+ (Siemens). Both programs were configured according to the defined boundary conditions and physical assumptions described in the previous section. The following part focuses on how the numerical setups were implemented, including the airflow fields, the definition of the injection parameters and the coupling of particles with the airflow field within the respective solver frameworks.

The main objective of the study is to investigate the particle filtering effect of venting tubes. Prior to the particle-resolved simulations, a preliminary airflow analysis was preformed using Meshfree to determine the steady-state conditions required for the particle transport simulations. The results showed that a steady state was fully achieved after about 0.4 seconds (with total physical time of 2 seconds) with no visible turbulence inside the venting tubes throughout the simulation (see Figure 1).

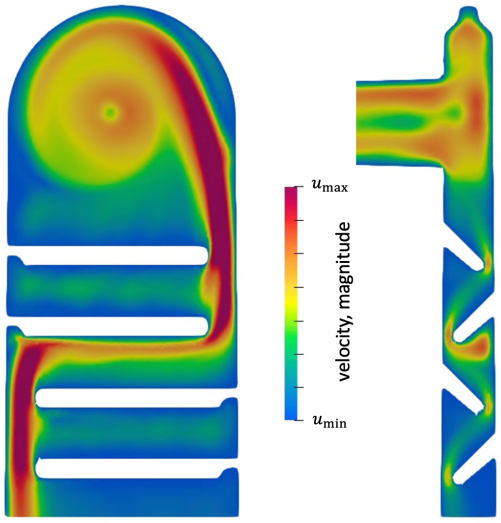

Figure 1: Airflow field generated by Meshfree

The Meshfree solver is based on the Finite Point Method (FPM) and operates without the need for mesh generation, which is often a time-consuming step in traditional CFD workflows. The program is particularly designed for particle simulations and is well suited for modeling particle–wall interactions, particle collisions, and slip or no-slip boundary conditions. To reach the conditions of the real system, several simulation iterations were performed. In the first step, the airflow field was internally calculated using Meshfree. In the second iteration, a frozen steady-state airflow field generated by STAR-CCM+ was imported into Meshfree. In the final iteration, an externally calculated airflow field from OpenFOAM (see Figure 2) was coupled with the Meshfree particle solver.

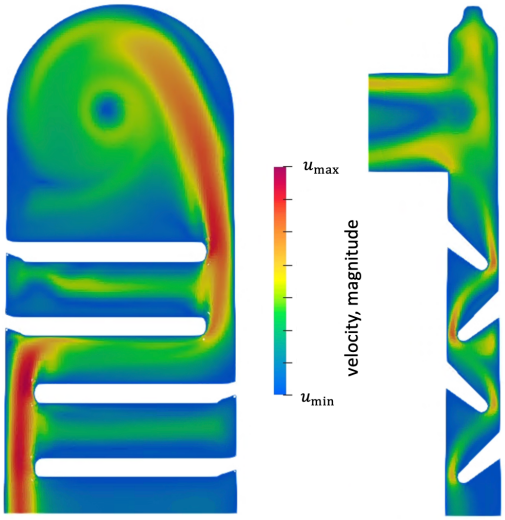

Figure 2: Airflow field generated by OpenFOAM

While the differences in simulation results between these approaches were insignificant, the computational performance varied significantly. The final iteration, based on the OpenFOAM airflow field, achieved a reduction in computation time of approximately 15 % compared to the other two setup variations. Such improvements in efficiency may be beneficial in large-scale studies where multiple components with similar configurations shall be simulated.

In all Meshfree simulations, the particle phase was solved using the Euler method (see section Methods and boundary conditions, p.3). By combining a mesh-free particle approach with a frozen steady-state airflow field, Meshfree offers a flexible and computationally efficient framework for analyzing particle transport under steady-state conditions.

The second program, STAR-CCM+, uses a Lagrangian particle tracking approach. A key limitation of this software is that externally generated airflow fields, such as those obtained from OpenFOAM, cannot be imported. As a result, the airflow field must be calculated

internally within StarCCM+. The results of this internal calculation are shown in

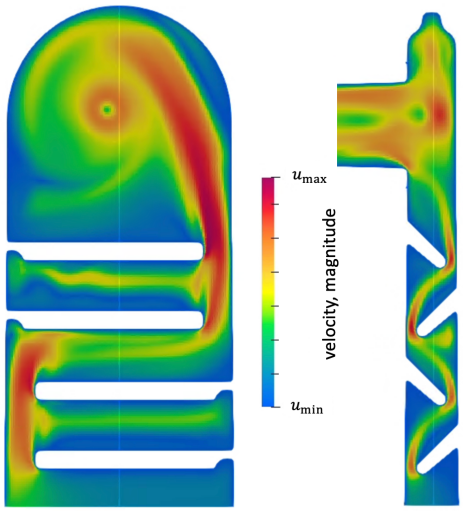

Figure 3. Compared to the OpenFOAM-generated airflow field, minor deviations were observed in the velocity distribution. These differences, however, may not significantly affect the predicted particle trajectories. allowing the particle transport behavior to be evaluated with sufficient accuracy. Since the main objective of this study is to examine the capability of both programs to represent particle transport phenomena, the internally generated airflow field in STAR-CCM+ was considered appropriate for the intended analysis.

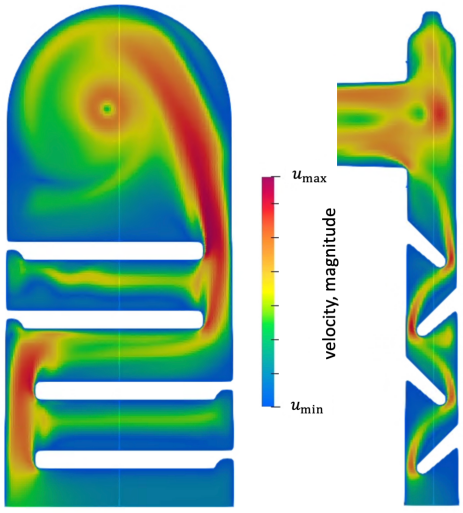

Figure 3: Airflow field generated by StarCCM+

STAR-CCM+ is particularly effective in resolving transient particle behavior and allows detailed representation of particle motion and flow characteristics. Despite these advantages, the airflow field predicted by both simulation tools shows generally similar characteristics. Minor deviations can be assigned to the fundamentally different numerical formulations employed by each method.

In the Eulerian framework, used by Meshfree, the airflow field is discretized in space and solved as a continuum, while particles are represented as concentrations within the control volumes of the computational domain. This method is computationally efficient and particularly suitable for large particle populations, although it provides less detailed information about individual particle trajectories (Zhang & Chen, 2007).

In contrast, the Lagrangian approach, applied in STAR-CCM+, explicitly tracks individual particles along their trajectories through the airflow field. This enables a detailed resolution of particle movement, wall collisions and residence time, but it comes with substantially higher computational costs. Particularly for simulations involving larger numbers of particles (Nordam et al, 2023).

Table 1 provides an overview about the properties of each simulation tool.

Table 1: Comparison of Meshfree and StarCCM+

Aspect	Meshfree (Fraunhofer)	StarCCM+ (Siemens)
Numerical method	Eulerian framework, Finite Point Method (FPM), Euler solver	Lagranian particle tracking
Mesh requirement	Mesh-free, no grid generation	Requires mesh of computational domain
Airflow field	Internal or external (e.g., OpenFOAM, StarCCM+); frozen fields applicable	Only internal airflow field calculation, no external import possible
Strengths	Flexible setup; efficient with frozen steady-state fields; suited for particle-wall, particle-particle interactions and slip/no-slip conditions	Accurate transient tracking; detailed particle trajectories, collisions
Limitations	Less detail for individual particle paths; accuracy depends on quality of airflow field	High cost for large particle numbers; restricted to internal airflow fields
Computational efficiency	Steady-state reached after approx. 0,4 s; OpenFOAM-based iteration approx. 15 % faster; transient coupling approx. five times longer	Efficient for transient runs but computationally demanding for high particle counts

Overall, the Eulerian and Lagrangian formulations have their specific advantages. The Eularian approach provides high computational efficiency and is more suited for capturing averaged concentration fields and bulk particle transport. In contrast Lagrangian models are more appropriate when particle-surface interactions or localized disposition phenomena are of interest with higher computational costs (Zhang & Chen, 2007; Azarpira et al., 2021).

By combining these two complementary methods, a more comprehensive understanding of particle transport and deposition within the venting tubes of

headlights was achieved. Meshfree offered valuable insights into steady-state particle–wall interactions, while STAR-CCM+ enabled the resolution of transient effects and inlet-driven particle distributions. This dual-tool approach allowed cross-validation of the numerical results and highlighted method-specific sensitivities, thereby increasing the reliability of the overall simulation study.

Experimental setup

Experimental test setups are required in cases where series components have technical limitations. In the present study, the focus lays on evaluating the filtration efficiency of venting tubes assembled in headlights. As these headlights are sealed components and cannot be opened without being damaged, thus, direct measurements of particles reaching the headlights are not possible.

To counteract these limitations, an appropriate experimental model was designed to reproduce the operating conditions of the venting system under controlled laboratory conditions. The use of such a model offers several advantages: it enables systematic variation of individual parameters (e.g., pressure difference and airflow rate), ensures reproducibility across multiple test iterations, and allows direct observation of the particle behavior.

To approximate the conditions inside automotive headlights, a simplified physical model was designed using a transparent acrylic glass box. This enables controlled boundary conditions. A schematic sketch of the experimental setup is provided in Figure 4.

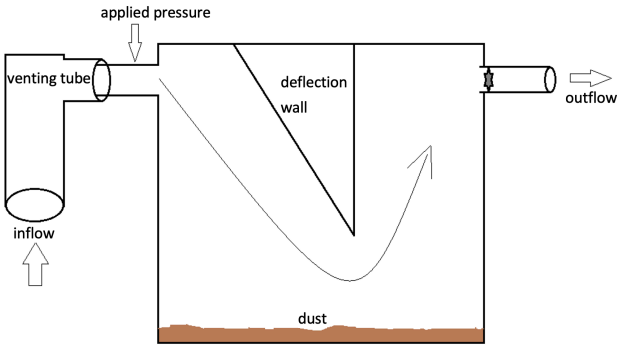

Figure 4: simplified model of the experimental setup

The venting tube was mounted on the inflow side of the acrylic glass box, where a defined pressure difference was applied to generate airflow through the system, with the outflow located on the opposite side. To influence the particle trajectories and enhance their deposition within the chamber, a deflection wall was installed. This element ensures that a significant part of the suspended dust can remain inside. After each test run, the deposited dust within the acrylic glass box was collected for quantitative analysis.

The current experimental setup is equipped with a volumetric flow sensor positioned at the outlet. This sensor enables continuous and precise monitoring of the airflow, with a minimum requirement of 1 l/min per venting element to ensure realistic operating conditions. Beyond simple flow measurement, the sensor also provides indirect information about pressure fluctuations occurring during the experiment. This is essential to ensure reproducibility and reliability, as it allows the operator to apply corrective adjustments in real time to stabilize the volumetric flow. Under these controlled conditions, dust samples were collected and have been analyzed in the laboratory to determine their particle size distribution using two laser diffraction techniques: the Fraunhofer and the Mie scattering method.

The Fraunhofer method is a laser diffraction technique in which a laser beam strikes a dispersed particle sample, causing the light to be diffracted by the particles. This method is well suited for the characterization of relatively large particles, typically above 10 µm . In contrast, the Mie method scatters laser light on dispersed particles and evaluates the measured angles of light intensity. Large particles scatter light at small angles, small particles at large angles, and this angle dependence of the scattered light intensity enables the particle size distribution to be calculated. This makes the Mie approach particularly suitable for the accurate determination of submicron and fine particle fractions (3P Instruments, 2019).

The comparative evaluation revealed that both methods produced consistent qualitative trends; however, the Mie-based results demonstrated closer consistency with the reference standards (see section “Results”) and provided higher accuracy across the relevant particle size range. Consequently, the Mie scattering method was selected as the preferred technique for further analysis.

Results

The results and key findings of the numerical and experimental studies are presented and discussed in the following section. The focus is placed on the particle transport behavior and the resulting filtration efficiency of the venting tubes. Followed by comparing the approaches to evaluate the predictive accuracy of the applied methods and to identify possible deviations between the experimental and numerical results.

As described in the section *Implementation of the Software* (page 4), a frozen steady-state airflow field

generated by OpenFOAM was used for the Meshfree simulation. For StarCCM+ the internally computed airflow field was used for the calculations. In addition to the fundamental forces considered in the particle motion equations (see section *Theoretical Background*, page 2), several boundary conditions had to be defined during the software implementation. These include the specification of the particle-wall interactions as well as the injection timing and location of the particles.

To ensure consistency across all simulation runs, the particle injection location was defined identically for all particle sizes. An injection plane was created at the same position in Meshfree and StarCCM+. Here the particles were injected at fixed coordinates following a predefined grid pattern to guarantees that particles enter the computational domain at identical positions in every simulation. This improves the reproducibility and comparability of the results.

The injection timing was selected to ensure that the system reached a steady-state condition prior to the particle injection. In Meshfree, this was implemented by introducing the particles after a short initialization period of several time steps, once the frozen airflow field was fully stabilized. In StarCCM+, particles were injected once a steady-state airflow field had been established, ensuring that the background flow remained unaffected by transient startup effects.

Figure 5 illustrates the particle injection configurations applied in Meshfree and StarCCM+. By imposing identical boundary conditions.

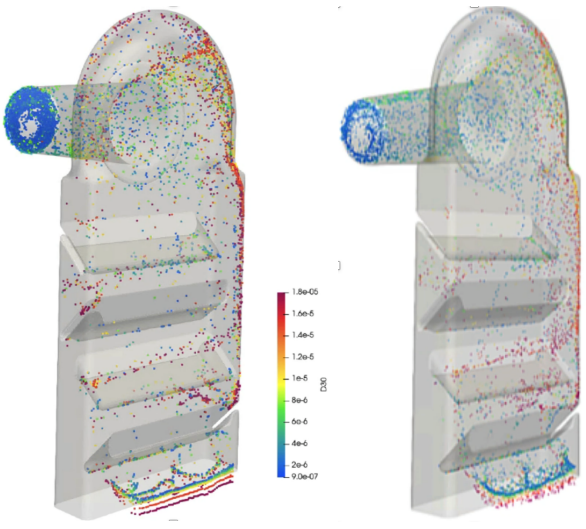

Figure 5: Particle flow: left Meshfree, right StarCCM+

To quantify the filter effect directly from the simulations, the number of particles were recorded at both the inlet and the outlet of the venting tube. From these data, the filtering effect could be determined according to the ratio of transmitted to injected particles. This method provides a stable and reproducible measure of the effective filtration behavior, representing the overall particle population across all size classes rather than relying on localized concentration fields.

The corresponding results for Meshfree and StarCCM+ are presented in Figure 6-

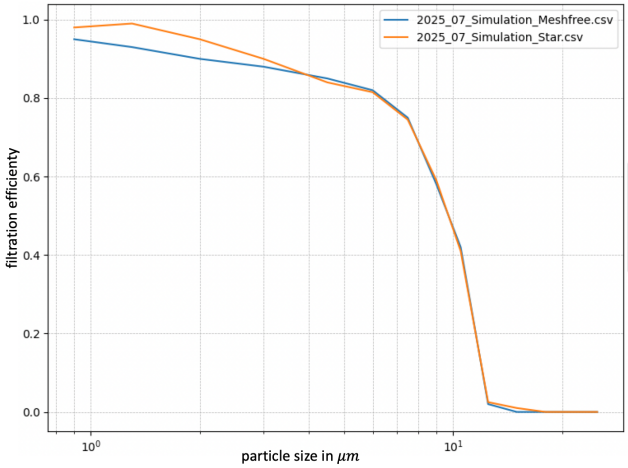

Figure 6: filtering effect, results of the simulation

Figure 6 shows the overall filter effect while Figure 5 illustrate the particle distribution within the system.

In general, the results are comparable. In StarCCM+, smaller particles have a little higher probability passing the venting tube compared to Meshfree. This deviation results possibly from the underlying numerical formulations: Star-CCM+ uses a Lagrangian particle tracking background, which resolves the trajectories of individual particles and may therefore predict a greater fraction of smaller particles. In contrast, Meshfree uses the Eulerian approach, which potentially leads to a more averaged description of small particle transport.

Small deviations in particle behavior can be observed between both simulation programs. However, the overall trend remains consistent. Larger particles are more effectively filtered within the venting tube due to their higher inertia, while smaller particles tend to remain coupled to the airflow field and are therefore more likely to pass through the venting tubes with the airstream. This behavior reflects the expected particle-flow interaction, in which inertial effects dominate for larger particles whereas aerodynamic drag primarily governs the motion of smaller particles. Despite these quantitative differences, both programs reproduce the same overall trend, indicating a consistent representation of the filter effect. The remaining deviations highlight the influence of the respective numerical methods on the predicted magnitude of particle transmission.

To validate the simulated predictions, laboratory measurements were done using the collected dust samples from the experimental setup. The resulting particle size distribution, and the cumulative volume distribution provided by the laboratory measurements, provide the experimental basis for comparing the results from the experiment and the numerical simulation.

To verify the reliability of the sampling and measurement procedure, reference dust samples were analyzed that had not been dispersed in the dust chamber. These reference measurements serve as a benchmark to determine whether the analyzed samples fall within a verifiable and reproducible range. According to ISO 12103-1, dust samples must conform to a defined reference distribution based on the Arizona Test Dust, which is categorized into several classes, such as A1 Ultrafine, A2 Fine, and A4 Coarse, each characterized by specific particle size ranges and cumulative distribution curves. In the present case, the A2 fine dust (labeled as 00_Norm_A2fine in Figure 7) applies. Compliance with these normative distributions ensures that the experimental samples are representative of standardized test conditions and that the measurement procedure yields verifiable results, as illustrated in Figure 7.

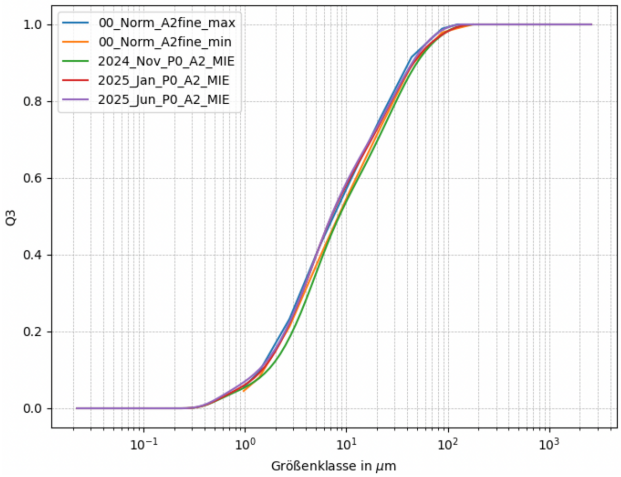

Figure 7: cumulative volume distribution $Q_3(x)$ over particle diameter, standardized dust

Figure 7 shows the comparison of three A2 fine reference samples with the particle size distribution specified in ISO 12103-1. The results illustrate that all three samples are within the normative range. This shows the reliability of the applied Mie scattering method and ensures that the following dust analyses are based on a validated and standardized measurement technique.

In the next step, further dust samples were extracted directly from the dust chamber and were compared with the ISO 12103-1 reference distribution to verify the homogeneous dispersion of the standardized test dust. This step was necessary to exclude a possible pre-filtration or deposition effect occurring before the actual venting tube experiments and that the samples represent a uniform input for further evaluation. The cumulative volume distributions of the dispersed dust within the chamber are illustrated in Figure 8.

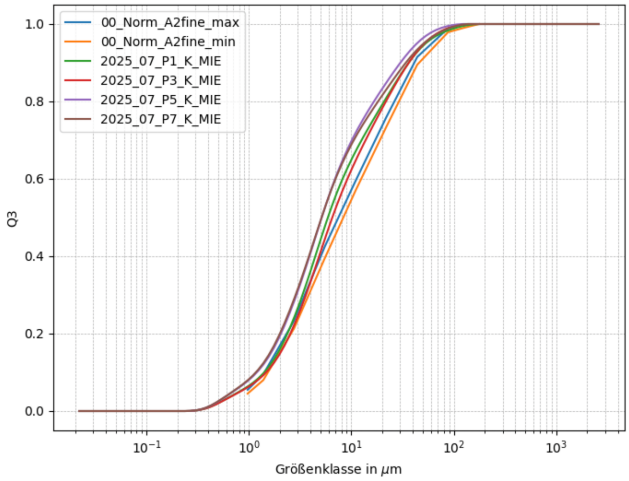

Figure 8: cumulative volume distribution $Q_3(x)$ over particle diameter, dust from the dust chamber

As shown in Figure 8, four samples taken from the dust chamber represent a distribution that shows a slight difference from the ISO 12103-1 reference curve. The chamber samples contain a higher proportion of smaller particles, which results in a shift of the cumulative volume distribution towards smaller particle sizes. Those results indicate that the ventilation within the dust chamber ensures in general a homogeneous dispersion of the test dust.

Once the dust chamber had been validated in terms of particle size distribution, experiments were continued using the acrylic glass box assembled with the venting tubes. The corresponding results are shown in Figure 9.

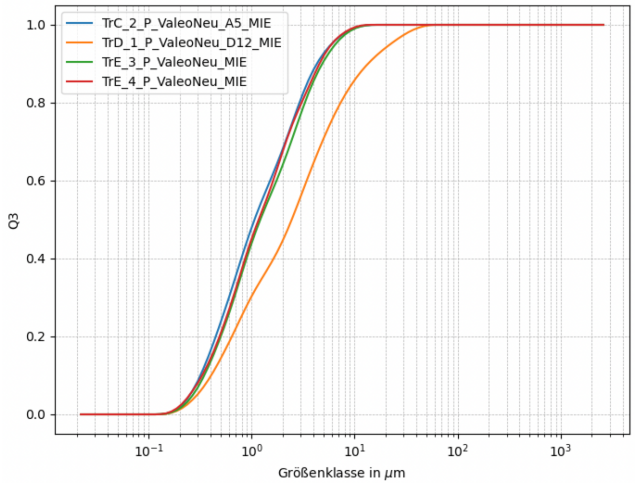

Figure 9: cumulative volume distribution $Q_3(x)$ over particle diameter, dust from the acrylic box with applied venting tubes

Figure 9 shows a selection of experiments conducted with one specific type of venting tube. Throughout the test series (labeled as TrB, TrC, TrD and TrE), several observations let to continuous adjustments of the experimental procedure. These modifications reflect the gradual optimization of the experimental setup, which resulted in more consistent and comparable results. As the optimization details are not the focus of this study, only general findings are discussed, providing the basis for the comparison between the experimental and numerical analyses.

Based on the characterization of the dust extracted from the dust chamber and the dust collected from the acrylic glass box assembled with the venting tube, the filter effect was determined. The data shown in Figure 7 and Figure 8 (page 8) served as the basis for the calculation. In this context, the dust sampled from the dust chamber was represents the input, while the dust collected inside the acrylic glass box serves as the output.

The filtering effect was calculated using equation 3 (see section *Theorical background*, page 2). The corresponding results are displayed in Figure 10.

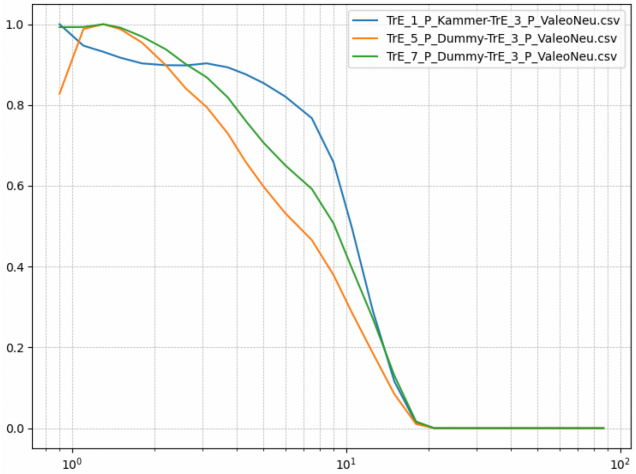

Figure 10: filtering effect, results from the experimental setup

An interesting aspect shown in Figure **10**, is that particles larger than approximately 20 µm do not pass through the venting tubes. This observation suggests that with increasing particle size, the particles cannot follow the airflow, probably due to their greater inertia and mass. As a result, they tend either to remain within the dust chamber or to deposit on the walls of the venting tubes itself. Physically, this behavior reflects the growing influence of inertial forces over aerodynamic drag as particle size increases. Consequently, the ability of coupling between the particles and the surrounding airflow reduces for larger particles, while smaller particles remain following the airflow. So, the smaller particles have a higher probability of transmission through the venting tube.

This result can also be interpreted in the context of the ISO 12103-1 standard, which specifies reference distributions for Arizona Test Dust used in experimental studies. The A2 Fine dust fraction used in these experiments contains a larger proportion of which particles below 20 µm , whereas coarser fractions include a higher number of larger particles that are effectively filtered within the system.

As a final step, the filtering effect from the experiment and the simulation were compared. This comparison is crucial for the validation of the applied models and to evaluate how accurate the different numerical approaches are in terms of predicting the filter effect of venting tubes. The results are shown in Figure 11.

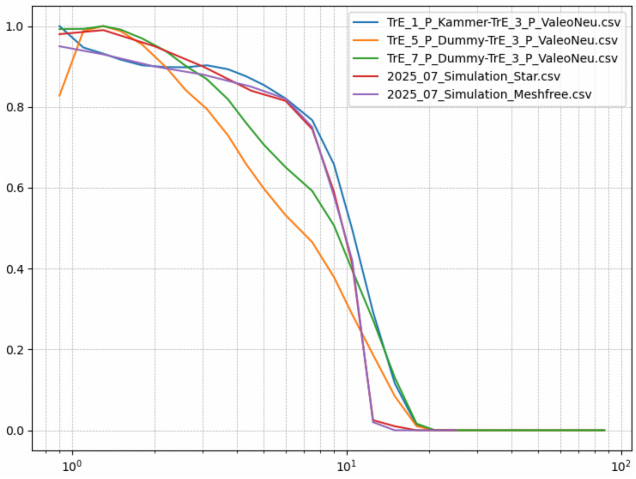

Figure 11: filtering effect, comparison of experiment and simulation

Figure 11 shows that the filtering effect received from the experiments deviates in part from the values predicted by the numerical simulations. Despite quantitative differences, the overall trend is consistent across both concepts. It can be observed that, within the

experiment and the simulation, no particles pass through the venting tube if their particle size is larger than approximately 20 µm. This reproducible border indicates that the dominant physical mechanism, the inability of larger particles to follow the airflow due to their higher mass, is captured correctly by both systems.

The comparison also shows that Meshfree and STAR-CCM+ successfully reproduce the general dependence of filtering effect on particle size. Quantitative deviations remain. In general, Meshfree tends to slightly underestimate the filtering possibility across most particle sizes, whereas STAR-CCM+ provides values that align more closely with the experimental results but is still not sufficient. The similarity of the results between the two simulation tools suggests that the observed differences are not mainly caused by the choice of solver but may rather be caused by physical effects that are difficult to fully capture numerically. Examples include particle agglomeration, adhesion to the venting tube surfaces, humidity within the dust chamber or electrostatic interactions could influence the effective filtering behavior under experimental conditions.

Taken together, the outcomes demonstrate that both numerical approaches are suitable for evaluating the filter effect of venting tubes and for reproducing the general particle-size-dependent behavior monitored in the experiments. At the same time, the deviations highlight that the predictive accuracy of simulations depends strongly on the completeness of the implemented physical models.

Conclusion

This study presented a combined experimental and numerical investigation of particle filtration behavior of venting tubes used in automotive headlights. The primary objective was to evaluate the capability of different simulation methods to predict particle transport and filtering effects of venting tubes within headlights and to compare these results with a specific experimental setup. An acrylic box with applied venting tubes was developed to reproduce a realistic airflow and dust distribution within a surrounded dust chamber under controlled laboratory conditions. The dust samples were analyzed regarding their particle size distribution.

Two complementary simulation tools were investigated: Meshfree (Fraunhofer) and STAR-CCM+ (Siemens). Both models were configured using identical physical assumptions, boundary conditions, and injection parameters to ensure comparability. The simulations were performed under a one-way coupling, in which the airflow phase influences the dispersed particles but not vice versa. Meshfree utilized an externally generated frozen steady-state airflow field from OpenFOAM, while STAR-CCM+ computed the corresponding flow internally. The particle motion was solved using a simplified form of the Basset–Boussinesq–Oseen (BBO) equation, considering only the dominant forces appropriate for quasi-steady flow conditions. Despite their different numerical formulations, Eulerian in Meshfree and Lagrangian in STAR-CCM+, both solvers reached comparable qualitative results for the airflow field and the particle transport.

The experimental observations showed that particles larger than approximately 20 µm were effectively filtered within the venting tube, suggesting that their mass prevents them from following the trajectory of the airflow. Smaller particles remained coupled to the airflow and have therefore a higher possibility to pass the venting tubes. Both simulation tools were able to reproduce this general trend. Quantitative deviations remain in both programs.

While the results from STAR-CCM+ provides values closer to the experimental data, Meshfree predicts lower particle transmission values across the size range. These differences highlight the influence of numerical formulations and simplifications on the predicted filtering behavior. The combination of both tools enables complementary analyses and provides a more accurate understanding of particle filtration mechanisms in venting tubes.

At the current stage, the predictive accuracy of the simulations is not yet sufficient to replace experimental validation. Ongoing experimental campaigns and continuous adaptations of the simulation setup aim to improve the comparability between both methods. This highlights the importance of systematic experimental reference data for validating computational models.

Future work should focus on integrating additional physical mechanisms, such as particle–particle interactions or wall adhesion phenomena. Incorporating these factors would enhance the predictive fidelity of the simulations and improve the approximation with experimental data. Furthermore, systematic studies of different venting tube geometries and filter materials could provide deeper insights into the influence of design parameters on dust behavior and airflow performance.

The experimental–numerical methodology developed in this study provides a robust foundation for future studies and represents a step toward establishing predictive, simulation-based design tools for particulate transport phenomena.

References

3P Instruments, 2019. Partikelgrößenanalyse – Von Gustav Mie bis zur neuesten Generation von Laserbeugungsgeräten. Partikelwelt, 20. Auszug. Neuburg: 3P Instruments. Available at: https://www.3p-instruments.com/wp-content/uploads/2021/05/PW20_dt_Auszug.pdf [Accessed: 15. July 2025].

Azarpira, M., Maghrebi, M.J., Dadvand, A. & Mirjalili, A., 2021. Comparison between Eulerian and Lagrangian approaches in the simulation of vortex flow. Applied Sciences, 11(5), 2267. Basel: MDPI.

Balachandar, S., & Eaton, J. K. (2010). Turbulent dispersed multiphase flow. Annual Review of Fluid Mechanics, 42, 111–133. https://doi.org/10.1146/annurev.fluid.010908.165243

Crown, C.T. 2005. Multiphase Flow Handbook. Boca Raton: CRC Press.

Crown, C. T., Schwarzkopf, J. D., Sommerfeld, M. & Tsuji, Y., 2011. Multiphase Flows with Droplets and Particles. Boca Raton: CRC Press.

Crowe, C. T., Schwarzkopf, J. D., Sommerfeld, M., & Tsuji, Y. (2012). Multiphase Flows with Droplets and Particles (2nd ed.). CRC Press.

Cussler, E. L. (2009). Diffusion: Mass Transfer in Fluid Systems (3rd ed.). Cambridge University Press. https://doi.org/10.1017/CBO9780511805134

Löffler, F. & Raasch, J., 1992. Grundlagen der Mechanischen Verfahrenstechnik. s.l.:Vieweg + Teubner.

Maxey, M. R., & Riley, J. J. (1983). Equation of motion for a small rigid sphere in a nonuniform flow. Physics of Fluids, 26(4), 883–889.

Michaelides, E. E. (1997). Review—The transient equation of motion for particles, bubbles, and droplets. Journal of Fluids Engineering, 119(2), 233–247.

Nordam, T., Mortensen, M., Pettersson Reif, B.A., & Vanneste, J., 2023. A comparison of Eulerian and Lagrangian implementations for selected example cases. Geoscientific Model Development, 16, pp. 5339-5355. Göttingen: Copernicus Publications.

Sommerfeld, P. D. -. I. M., 2000. Theoretical and Experimental Modelling of Particulate Flows, Halle: Karman Institute for Fluid Dynamics

Stieß, M. (2009). Mechanische Verfahrenstechnik – Partikeltechnologie 1: Grundlagen und Verfahren. 3rd ed. Berlin: Springer Vieweg.

Zhang, Z. & Chen, Q., 2007. Comparison of the Eulerian and Lagrangian methods for predicting particle transport in enclosed spaces. Atmospheric Environment, 41(25), pp. 5236-5248.